We are IntechOpen,
the world's leading publisher of
Open Access books
Built by scientists, for scientists

6,900
Open access books available

186,000
International authors and editors

200M
Downloads

154
Countries delivered to

Our authors are among the

TOP 1%
most cited scientists

12.2%
Contributors from top 500 universities

CLARIVATE ANALYTICS

BOOK CITATION INDEX

INDEXED

WEB OF SCIENCE™

Selection of our books indexed in the Book Citation Index
in Web of Science™ Core Collection (BKCI)

Interested in publishing with us?
Contact book.department@intechopen.com

Numbers displayed above are based on latest data collected.
For more information visit www.intechopen.com

High Performance Holographic Polymer Dispersed Liquid Crystal Systems Formed with the Siloxane-containing Derivatives and Their Applications on Electro-optics

Yeonghee Cho and Yusuke Kawakami
Japan Advanced Institute of Science and Technology
Japan

1. Introduction

Holography is a very powerful technology for high density and fast data storage, which have been applied to the systems known as holographic polymer dispersed liquid crystal (HPDLC), in which gratings are formed by anisotropic distribution of polymer and LC-rich layers through photopolymerization of monomers or oligomers and following phase separation of LC in the form of interference patterns of incident two laser beams [1-5]. Much attentions have been attracted to HPDLC systems due to their unique switching property in electric field to make them applicable to information displays, optical shutters, and information storage media [6-15].

Many research groups have made efforts to realize useful recording materials for high performance holographic gratings [16-18]. Photo-polymerizable materials, typically multi-functional acrylates, epoxy, and thiol-ene derivatives have been mostly studied because of their advantages of optical transparency, large refractive index modulation, low cost, and easy fabrication and modification[19-25]. T.J. Bunning group has reported investigation that the correlation between polymerization kinetics, LC phase separation, and polymer gel point in examining thiol-ene HPDLC formulations to enable more complete understanding of the formation of thiol-ene HPDLCs [26]. Kim group has developed that the doping of conductive fullerene particles to the formulations based on polyurethane acrylate oligomers in order to reduce the droplet coalescence of LC and operating voltage [27].

Further extensive research has been devoted to the organic-inorganic hybrid materials having the sensitivity to visible laser beam to resolve the drawbacks of photopolymerizable materials such as volume shrinkage, low reliability, and poor long term stability even high reactivity of them as well waveguide materials, optical coatings, nonlinear optical materials, and photochromic materials [28-29]. Blaya et al. theoretically and experimentally analyzed the angular selectivity curves of nonuniform gratings recorded in a photopolymerizable silica glass due to its rigidity suppressing the volume shrinkage [30]. Ramos et al. found that a chemical modification of the matrix with tetramethylorthosilicate noticeably attenuates the shrinkage, providing a material with improved stability for permanent data storage applications [31].

However, those materials still have significant drawbacks such as volume shrinkage, low reliability, and poor long term stability.

Recently, we have focused on the siloxane-containing derivatives by taking advantage of their chemical and physical properties with high thermal stability, high optical clarity, flexibility, and incompatibility[32].

In this research, first, siloxane-containing epoxides were used to induce the efficient separation of LC from polymerizable monomer and to realize high diffraction efficiency and low volume shrinkage during the formation of gratings since the ring-opening polymerization (ROP) systems with increased excluded free-volume during the polymerization suppress the volume shrinkage [33]. Although various epoxide derivatives were used, cyclohexane oxide group should be more suitable to control the volume shrinkage in the polymerization due to their ring structure with more bulky group. Actually, we improved the volume shrinkage causing a serious problem during the photopolymerization, by using the ROP system with novel siloxane-containing spiroorthoester and bicyclic epoxides.

Generally, the performance of holographic gratings in HPDLC systems strongly depends on the final morphologies, sizes, distribution, and shapes of phase-separated LC domains controlled by adjusting the kinetics of polymerization and phase separation of LC during the polymerization. Control of the rate and density of cross-linking in polymer matrix is very important in order to obtain clear phase separation of LC from polymer matrix to homogeneous droplets. Too rapid initial cross-linking by multi-functional acrylate makes it difficult to control the diffusion and phase separation of LC. At the same time, high ultimate conversion of polymerizable double bond leading to high cross-linking is important for long-term stability.   These are not easy to achieve at the same time.

Till now optimization of cross-linking process has been mainly pursued by controlling the average functionality of multi-functional acrylate by mixing dipentaerythritol pentaacrylate (DPEPA), trimethylolpropane triacrylate (TMPTA) and tri(propyleneglycol) diacrylate, or by diluting the system with mono-functional vinyl compound like 1-vinyl-2-pyrollidone (NVP) [34-37]. In case of TMPTA, considerably high concentration was used. Mono-functional NVP adjusts the initial polymerization rate and final conversion of acrylate functional groups by lowering the concentration of cross-linkable double bonds [38]. However, the effects were so far limited, and these systems still caused serious volume shrinkage and low final conversion of polymerizable groups.   Thus, the gratings are not long-term stable, either.   Moreover, the phase separation of LC component during the matrix formation was governed only by its intrinsic property difference against polymer matrix, accordingly not well-controlled. These systems could be called as "passive grating formation" systems.

Thus, if we consider the structure and reactivity of siloxane compounds in relation with the property, it will be possible to propose new systems to improve the performance of HPDLC gratings.

Second, the objective of this research is to show the effectiveness of the simultaneous siloxane network in formation of polymer matrix by radically polymerizable multi-functional acrylate by using trialkoxysilyl (meth)acrylates, and to characterize the application of dense wavelength division multiplexing (DWDM) systems. By loading high concentration of trialkoxysilyl-containing derivatives, volume shrinkage during the formation of polymer matrix should be restrained.   The principal role of multi-functional

acrylate in grating formation is to make the LC phase-separate by the formation of cross-linked polymer matrix.

Our idea is to improve the property of gratings through importing the siloxane network in polymer matrix, by not only lowering the contribution of initial rapid radical cross-linking of TMPTA and realizing complete conversion of double bonds, but also maintaining the desirable total cross-linking density assisted by hydrolysis-condensation cross-linking of trialkoxysilyl group in the (meth)acrylate component to control the phase separation of LC from polymer matrix [39]. Such cross-linking can be promoted by the proton species produced from the initiating system together with radical species by photo-reaction [40-42]. In our system, phase separation of LC is not so fast compared with simple multi-functional acrylate system, and secondary cross-linking by the formation of siloxane network enforce the LC to completely phase-separate to homogeneous droplets, and high diffraction efficiency could be expected. We named this process as "proton assisted grating formation".

These systems should provide many advantages over traditional systems induced only by radical polymerization by improving: 1) the volume shrinkage by reducing the contribution of radical initial cross-linking by importing the siloxane network in whole polymer networks, 2) the contrast of siloxane network formed by the hydrolysis of ω-methacryloxyalkyltrialkoxysilane against polymer matrix, and 3) the stability of final gratings via combination of the characteristics of siloxane gel and rather loosely cross-linked radically polymerized system.

Finally, poly (propylene glycol) (PPG) derivatives functionalized with triethoxysilyl, hydroxyl, and methacrylate groups were synthesized to control the reaction rate and extent of phase separation of LC, and their effects were investigated on the performance of holographic gratings. The well-constructed morphology of the gratings was evidenced by atomic force microscopy (SEM).

2. Experimental

2.1 Holographic recording materials

Multi-functional acrylates, trimethylolpropane triacrylate (TMPTA) and dipentaerythritol penta-/hexa- acrylate (DPHA), purchased from Aldrich Chemical Co., were used as radically cross-linkable monomers to tune the reaction rate and cross-linking density.

Structures of ring-opening cross-linkable monomers used in this study are shown in **Figure 1**. Bisphenol-A diglycidyl ether (A), neopentyl glycol diglycidyl ether (B), bis[(1,2-epoxycyclohex-4-yl)methyl] adipate (F) from Aldrich Chemical Co. and 1,3-bis(3-glycidoxypropyl)-1,1,3,3-tetramethyldisiloxane (C), 1,5-bis(glycidoxypropyl)-3-phenyl-1,1,3,5,5-pentamethyltrisiloxane (E) from Shin-Etsu Co. were used without further purification. 1,5-Bis(glycidoxypropyl)-1,1,3,3,5,5-hexamethyltrisiloxane (D), 1,3-bis[2-(1,2-epoxycyclohex-4- yl)ethyl]-1,1,3,3-tetramethyldisiloxane (G), and 1,5-bis[2-(1,2-epoxycyclohex-4-yl)ethyl]- 1,1,3,3,5,5-hexamethyltrisiloxane (H) were synthesized by hydrosilylation of allyl glycidyl ether, or 4-vinyl-1-cyclohexene-1,2-epoxide (Aldrich Chemical Co.) with 1,1,3,3,5,5-hexamethyltrisiloxane, or 1,1,3,3-tetramethyldisiloxane (Silar Laboratories) in toluene at 60~70°C for 24h in the presence of chlorotris(triphenylphosphine)rhodium(I) [RhCl(PPh3)3] (KANTO chemical co. Inc.).

Methacryloxymethyltrimethylsilane (M_M-TMS), methacryloxymethyltrimethoxysilane (M_M-TMOS), 3-methacryloxypropyltrimethoxysilane (M_P-TMOS), 3-methacryloxypropyltriethoxysilane (M_P-TEOS), 3-N-(2-

methacryloxyethoxycarbonyl)aminopropyltriethoxysilane (M_U-TEOS), and 3-N-(3-methacryloxy-2-hydroxypropyl)aminopropyltriethoxysilane (M_H-TEOS), purchased from Gelest, Inc., were used as reactive diluents (**Figure 2**). Methacrylate with trialkoxysilane are capable of not only radical polymerization but also hydrolysis-condensation.

To investigate the effects of functional groups of photo-reactive PPG derivatives on performance of holographic gratings, three types of PPG derivatives were functionalized with triethoxysilyl, hydroxyl, and methacrylate groups as shown in **Figure 3**. PPG derivative with difunctional triethoxysilyl groups (PPG-DTEOS) and PPG derivative together with hydroxyl and triethoxysilyl groups (PPG-HTEOS) were synthesized by using 1 mol of PPG (Polyol.co. Ltd.) with 2 mol and 1 mol of 3-(triethoxysilyl)propyl isocyanate (Aldrich), respectively. PPG derivative together with methacrylate and triethoxysilyl groups PPG-MTEOS was synthesized by using 1 mol of PPG-HTEOS with 1 mol of 2-isocyanatoethyl methacrylate (Gelest, Inc.).

 1-Vinyl-2-pyrrolidone (NVP) was used as another radically polymerizable reactive diluent. Commercial nematic LC, TL203   (T_{NI}=74.6 °C, n_e=1.7299, n_o=1.5286, Δn=0.2013) and E7 (T_{NI}=61 °C, n_e=1.7462, n_o=1.5216, Δn=0.2246) , purchased from Merck & Co. Inc., were used without any purification.

2.2 Composition of photo-initiator system and recording solution

Photo-sensitizer (PS) and photo-initiator (PI) having sensitivity to visible wavelength of Nd-YAG laser (λ= 532 nm) selected for this study are 3, 3'-carbonylbis(7-diethylaminocoumarin) (KC, Kodak) and diphenyliodonium hexafluorophosphate (DPI, AVOCADO research chemicals Ltd.), respectively, which produce both cationic and radical species [43-45]. The concentrations of the PS and PI were changed in the range of 0.2-0.4 and 2.0-3.0 wt % to matrix components, respectively.

Recording solution was prepared by mixing the matrix components (65 wt%) and LC (35 wt%), and injected into a glass cell with a gap of 14 μm and 20 μm controlled by bead spacer.

2.3 Measurement of photo-DSC and FTIR

The rate of polymerization was estimated from the heat flux monitored by photo-differential scanning calorimeter (photo-DSC) equipped with a dual beam laser light of 532nm wavelength. Matrix compounds were placed in uncovered aluminum DSC pans and cured with laser light by keeping the isothermal state of 30 °C at various light intensities.

Infrared absorption spectra in the range 4000-400 cm-1 were recorded on polymer matrix compounds by Fourier Transform Infrared Spectroscopy (FTIR) (Perkin-Elmer, Spectrum One).

2.4 Optical setup for transmission holographic gratings

Nd:YAG solid-state continuous wave laser with 532 nm wavelength (Coherent Inc., Verdi-V2)   was used as the irradiation source as shown in Figure 4.

The beam was expanded and filtered by spatial filters, and collimated by collimator lens. s-Polarized beams were generated and split by controlling the two λ/2 plates and polarizing beam splitter. Thus separated two s-polarized beams with equal intensities were reflected by two mirrors and irradiated to recording solution at a pre-determined external beam angle (2θ) which was controlled by rotating the motor-driven two mirrors and moving the rotation stage along the linear stage. In this research, the external incident beam angle was fixed at 16° (2θ) against the line perpendicular to the plane of the recording cell.

Real-time diffraction efficiency was measured by monitoring the intensity of diffracted beam when the shutter was closed at a constant time interval during the hologram recording. After the hologram was recorded, diffraction efficiency was measured by rotating the hologram precisely by constant angle by using motor-driven controller, with the shutter closed to cut-off the reference light, to determine the angular selectivity. Holographic gratings were fabricated at 20mW/cm² intensity for one beam, and the optimum condition was established to obtain the high diffraction efficiency, high resolution, and excellent long-term stability after recording. Diffraction efficiency is defined as the ratio of diffraction intensity after recording to transmitting beam intensity before recording.
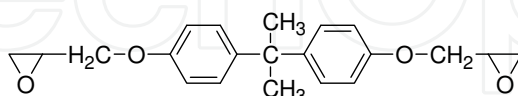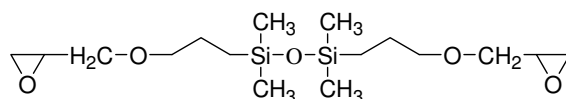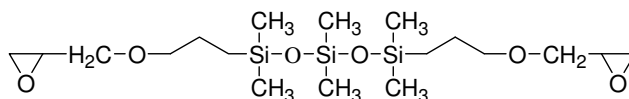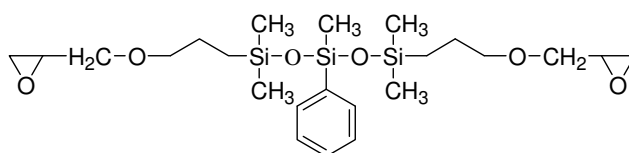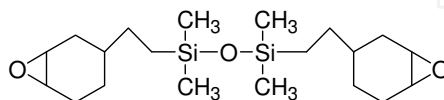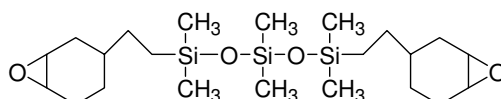
Bisphenol A diglycidy lether (**A**)
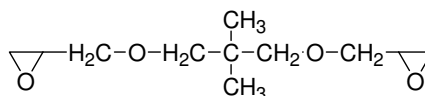
Neopentylglycol diglycidyl ether (**B**)

1,3-Bis(3-glycidoxypropyl)-1,1,3,3-tetramethyldisiloxane (**C**)

1,3-Bis(3-glycidoxypropyl)-1,1,3,3,5,5-hexamethyltrisiloxane (**D**)

1,5-Bis(3-glycidoxypropyl)-3-phenyl-1,1,3,5,5-pentamethyltrisiloxane (**E**)

Bis[(1,2-epoxycyclohex-4-yl)methyl] adipate (**F**)

1,3-Bis[2-(1,2-epoxycyclohex-4-yl)ethyl]-1,1,3,3-tetramethyldisiloxane (**G**)

1,5-Bis[2-(1,2-epoxycyclohex-4-yl)ethyl]-1,1,3,3,5,5-hexamethyltrisiloxane (**H**)

Fig. 1. Chemical structures of ring-opening cross-linkable monomers.
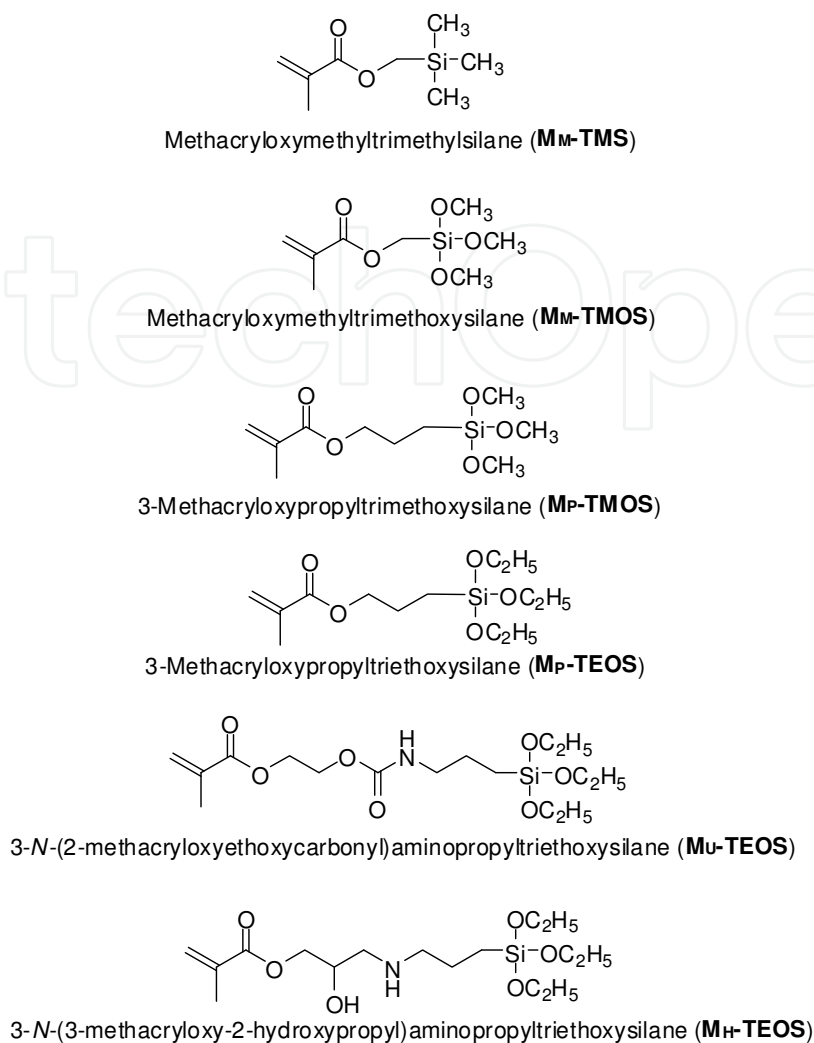
Methacryloxymethyltrimethylsilane (**MM-TMS**)

Methacryloxymethyltrimethoxysilane (**MM-TMOS**)

3-Methacryloxypropyltrimethoxysilane (**MP-TMOS**)

3-Methacryloxypropyltriethoxysilane (**MP-TEOS**)

3-*N*-(2-methacryloxyethoxycarbonyl)aminopropyltriethoxysilane (**MU-TEOS**)

3-*N*-(3-methacryloxy-2-hydroxypropyl)aminopropyltriethoxysilane (**MH-TEOS**)

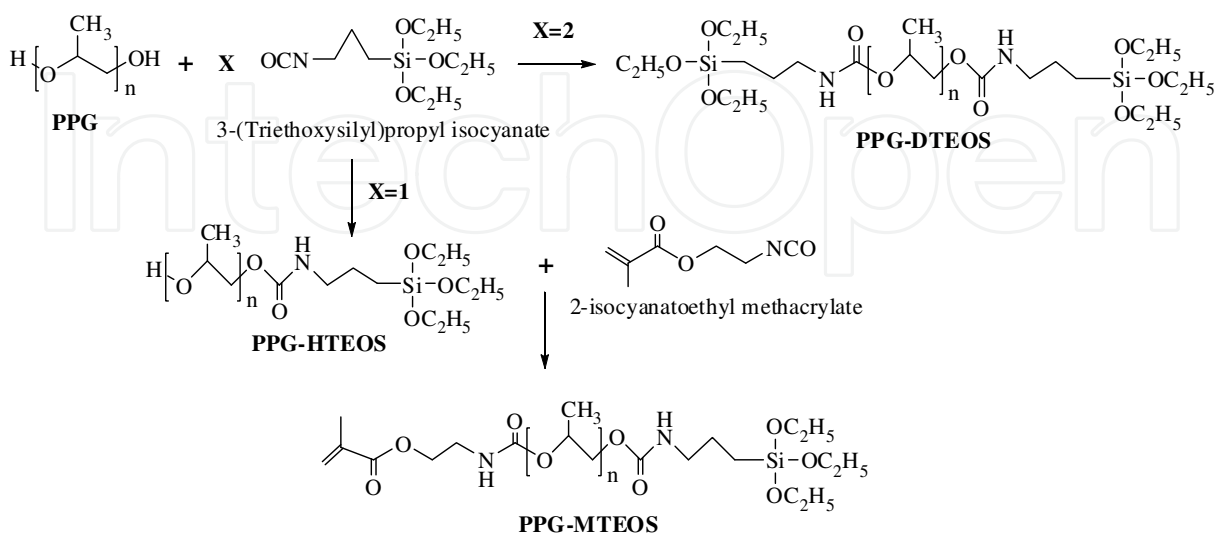Fig. 2. Structures of ω-methacryloxyalkyltri-alkyl or -alkoxysilanes.

Fig. 3. Chemical structures of PPG derivatives functionalized with triethoxysilyl, hydroxyl, and methacrylate groups as polymer matrix components.
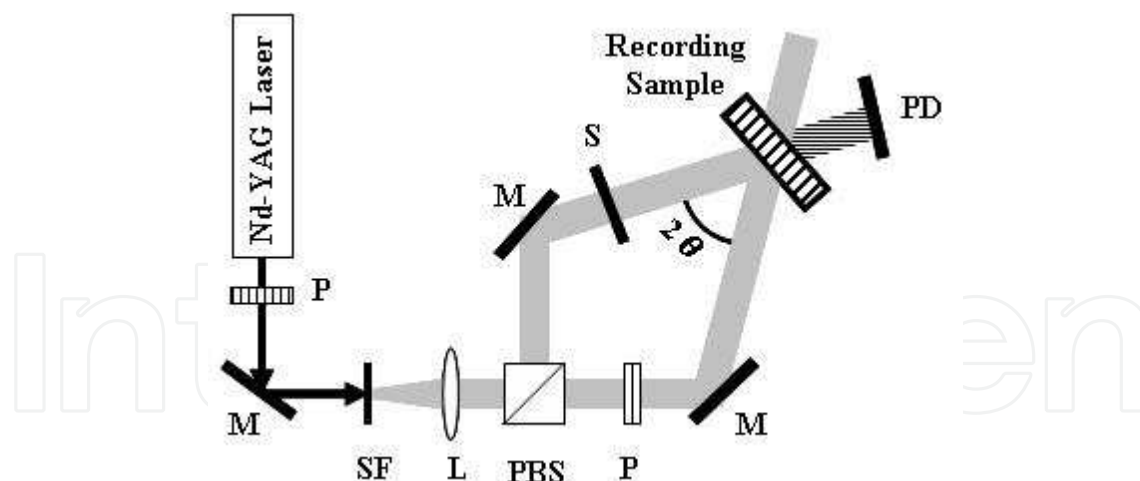
Fig. 4. Experimental setup for the holographic recording and real-time reading; P: 1/2λ
plate, M: mirror, SF: spatial filter, L: collimating lens, PBS: polarizing beam splitter, S:
shutter, 2θ: external inter-beam angle, PD: power detector.

2.5 Morphology of holographic gratings

Surface morphology of gratings was examined with scanning electron microscope (SEM,
HITACHI, S-4100). The samples for measurement were prepared by freeze-fracturing in liquid
nitrogen, and washed with methanol for 24h to extract the LC, in case necessary. Exposed
surface of the samples for SEM was coated with a very thin layer of Pt-Pd to minimize artifacts
associated with sample charging (HITACHI, E-1030 ion sputter). Surface topology of
transmission holographic grating was examined with atomic force microscopy (AFM,
KIYENCE, VN8000). The samples for measurement were prepared by freeze-fracturing in
liquid nitrogen, and washed with methanol for 24h to extract the LC. AFM having a contact
mode cantilever (KIYENCE, OP-75042) was used in tapping mode for image acquisition.

3. Results and discussion

3.1 Effects of siloxane-containing bis(glycidyl ether)s and bis(cyclohexene oxide)s on the real-time diffraction efficiency

Real-time diffraction efficiency, saturation time, and stability of holographic gratings
according to exposure time were evaluated. Figure 5 shows the effects of chemical structures
of bis(glycidyl ether)s (A - E) on real-time diffraction efficiency at constant concentration of
E7 (10 wt %) in recording solution [DPHA : NVP : (A - E) = 50: 10: 40 relative wt %].
In general, high diffraction efficiency can be obtained by the formulation of recording
solution with large difference in refractive indexes between polymer matrix and LC, and by
inducing the good phase separation between polymer rich layer and LC rich layer. As
expected, gratings formed with C having siloxane component had remarkably higher
diffraction efficiency than gratings formed with A and B without siloxane component,
which seemed to have resulted from effects of siloxane component to induce good phase
separation of E7 from polymer matrix toward low intensity fringes by its incompatible
property against E7. Longer induction period for grating formation of C was attributed to
lower viscosity of recording solution, and the diffraction efficiency gradually increased and
reached to higher value, which resulted from the further phase separation of E7 due to the
flexible siloxane chain that helped migration of E7 toward low intensity fringes.
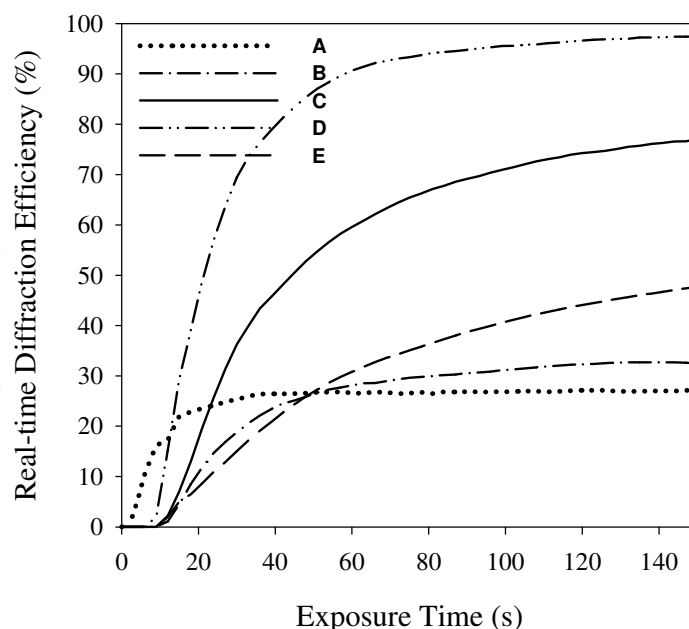
Fig. 5. Real-time diffraction efficiency of the gratings formed with (A - E) with 10 wt % E7 [DPHA: NVP: (A - E) = 50: 10: 40 relative wt %].

All the gratings formed with (C – E) having siloxane component showed high diffraction efficiencies. The highest diffraction efficiency 97% was observed for D with trisiloxane chain, probably due to its incompatible property with E7. However, gratings formed with E, having phenyl group in the trisiloxane chain, showed the lowest diffraction efficiency. Bulky phenyl group attached in the siloxane chain reduced the flexibility of the chain to result in the suppression of phase separation. It might have contributed to the increase of the interaction between polymer matrix with E7 having bi-/terphenyl group.

 Figure 6 shows the real-time diffraction efficiency of the gratings formed with bis(cyclohexene oxide) derivatives (F - H) at constant concentration of E7 (10 wt %) [DPHA: NVP: (F - H) = 50: 10: 40 relative wt %].

Gratings formed with G and H having siloxane component had higher diffraction efficiency than F without it, which seemed to indicate that, as mentioned above, siloxane chain in G and H made the solution less viscous, and incompatible with E7, which helped the easy diffusion and good phase separation between polymer matrix and E7 to result in high refractive index modulation, n. Especially, H showed higher diffraction efficiency than E, probably due to flexibility and incompatibility brought about by its longer siloxane chain. However, compared with C and D, G and H did not give higher diffraction efficiency, even with longer siloxane chain. This may be understood because of the difference in the chemical structure of ring-opening cross-linkable group. G and H have bulkier cyclohexene oxide as functional group and have higher viscosity, accordingly its diffusion toward high intensity fringes seems difficult compared with that of C or D.

3.2 Volume shrinkage of the gratings depending on the structure of bis(epoxide)
Photo-polymerizable system as holographic recording material usually causes significant volume shrinkage during the formation of gratings, which can distort the recorded fringe pattern and cause angular deviations in the Bragg profile. Therefore, it is very important to solve the problem of volume shrinkage in photopolymerization systems.
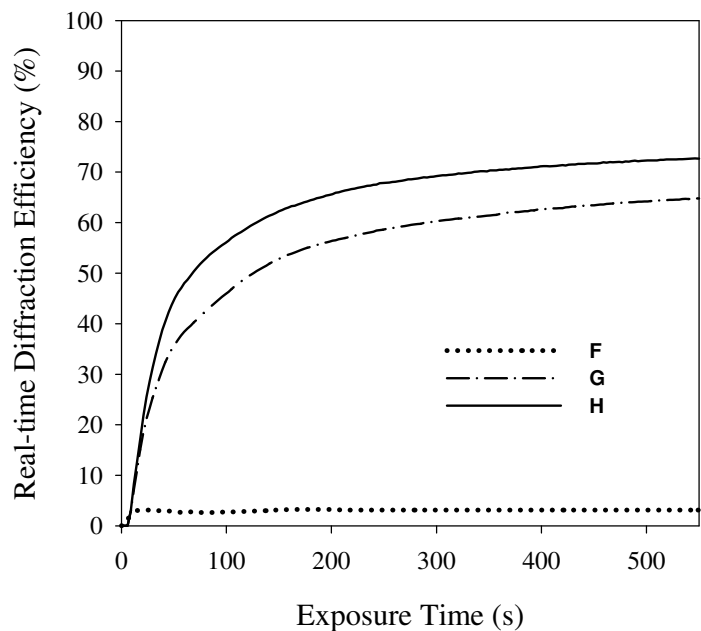
Fig. 6. Real-time diffraction efficiency of the gratings formed with (F – H) and 10 wt % E7
[DPHA: NVP: (F - H) = 50: 10: 40 relative wt %].

For the measurement of volume shrinkage, slanted holographic gratings were fabricated by
simply changing the angles of reference (R) and signal (S) beams, as shown in Figure 7 [46].
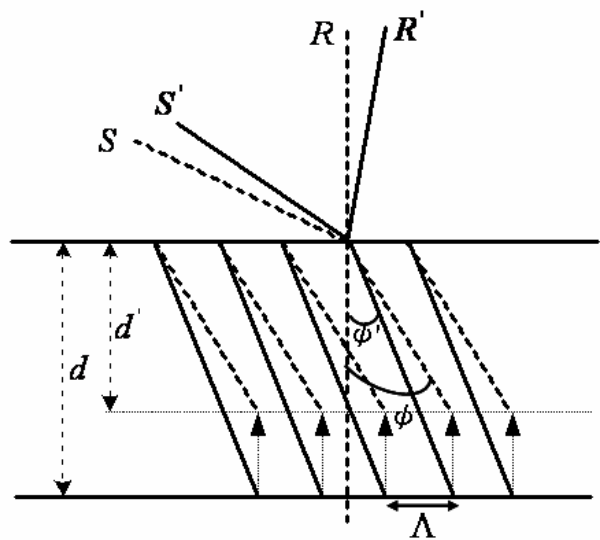

Fig. 7. Fringe-plane rotation model for slanted transmission holographic recording to
measure the volume shrinkage.

R and S are recording reference (0°) and signal (32°) beams. φ (16° in this study) is the
slanted angle against the line perpendicular to the plane of the recording cell of gratings
formed with S and R. Solid line in the grating indicates the expected grating. d is the sample
thickness. Actual grating formed by S and R was deviated from the expected grating shown
by dashed line by volume shrinkage of the grating. Presumed signal beam (S'), which
should have given actual grating was detected by rotating the recorded sample with

reference light R off. This rotation of angle was taken as deviation of slanted angle. R' and S' are presumed compensation recording reference and signal beams. φ' is the slanted angle in presumed recording with S' and R', and d' is the decreased sample thickness caused by volume shrinkage. Degree of volume shrinkage can be calculated by following equation;

$$\text{Degree of volume shrinkage} = 1 - \frac{d'}{d} = 1 - \frac{\tan \varphi'}{\tan \varphi} \quad (\tan \varphi' = \frac{\Lambda}{d}, \tan \varphi = \frac{\Lambda}{d'}) \quad (1)$$

Figure 8 shows the angular deviations from the Bragg profile of the gratings formed with C and G having bis(glycidyl ether) and bis(cyclohexene oxide), respectively, at constant concentration of E7 (10 wt %) [DPHA : NVP: (C or G) = 50: 10: 40 relative wt%]. The angular shifts from the Bragg matching condition (0 degree) at both positions of diffracted R and S beams indicates the extent of volume shrinkage of the gratings. Grating prepared from the recording solution containing only radically polymerizable compounds [DPHA : NVP = 50: 50 in relative wt%] was used as the reference.
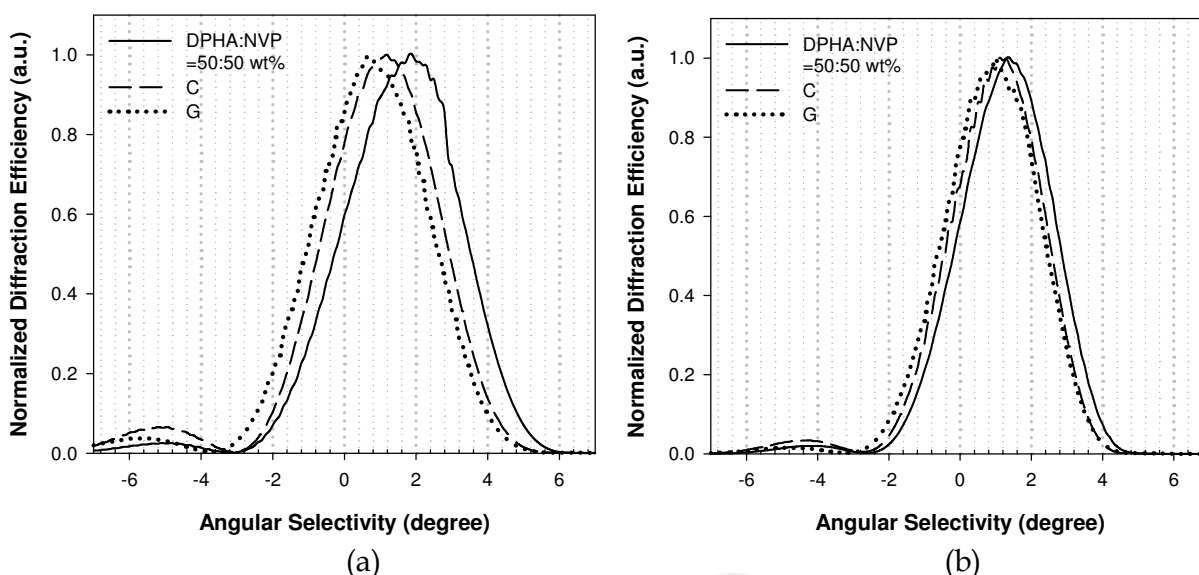

Fig. 8. Angular deviation from the Bragg profile for the gratings formed with C and G [DPHA: NVP : (C or G) = 50: 10: 40 relative wt %] detected by (a) diffracted S beam, and (b) diffracted R beam.

As shown in Figure 8, gratings formed with G having bis(cyclohexene oxide) showed smaller deviation from Bragg matching condition than gratings formed with C having bis(glycidyl ether) for both diffracted R and S beams. The diffraction efficiency after overnight was only slightly changed, which indicated the volume shrinkage after overnight was negligible.

Diffraction efficiency, angular deviation, and volume shrinkage of each system were summarized in Table 1.

Gratings formed with only radically polymerizable multifunctional acrylate (DPHA: NVP = 50:50 relative wt %) showed the largest angle deviation, and the largest volume shrinkage of 10.3% as is well known. Such volume shrinkage could be reduced by combining the ring-

opening cross-linkable monomers. Especially, bis(cyclohexene oxide)s were effective to reduce the volume shrinkage (5.6 %), probably due to its cyclic structure, although their diffraction efficiency was lower than those formed with bis(glycidyl ether)s.

Recording solution	Diffraction efficiency (%)a	Angular deviation of diffracted		φ'	Degree of volume shrinkage (%)
		S beam (degree)	R beam (degree)		
DPHA: NVP =50:50 wt %	2	1.8	1.35	14.42	10.3
DPHA: NVP : C = 50: 10: 40 wt %	47	1.2	1.1	14.85	7.5
DPHA: NVP: G = 50:10:40 wt %	29	0.7	1.0	15.15	5.6
DPHA: NVP : D = 50: 10: 40 wt %	54	0.83	0.76	15.21	5.2
DPHA: NVP: H = 50:10:40 wt %	31	0.66	0.70	15.32	4.5

Table 1. Deviations from Bragg angle of diffracted S and R beams (degree) and degree of volume shrinkage and diffraction efficiency determined by S beama.

The shrinkage effect could be caused by mechanical reduction of the grating pitch and a real time change in refractive index of the irradiated mixture. Which factor is playing a major role is not clear at present. Distinction of these factors will be a future problem.

One of the possible reasons for small volume shrinkage is the effective formation of IPN structure in the grating in the recording system DPHA : NVP : G = 50: 10: 40 relative wt %. The balance between the formation of initial cross-linking of DPHA and following cross-linking by G might be proper to produce effective IPN structure.

Good evidence for these was shown in Figure 9 of SEM morphologies.

Figure 9 (a) and (c) show clearly phase-separated polymer layers after the treatment with methanol, which means almost perfect phase separation between polymer rich layers and E7 rich layers. Cross-sectional and surface views of the sample could be observed. When 20 wt % E7 was used, a little incompletely phase separated E7 layers were shown in Figure 9 (d), although much higher E7 was phase separated than the case of 5 wt % E7 [Figure 9 (b)]. Grating spacing was close to the calculated value from the composition of recording solution for the grating prepared with 5 wt % E7.

3.3 Angular selectivity

When the multiplex hologram recording is required, it is necessary to know the angular selectivity. The smaller the value, the more multiplex data or gratings can be recorded [47-49]. Angular selectivity ($\Delta\theta_{ang}$) is defined by Kogelnik's coupled wave theory as follows [50]:

$$\Delta\theta_{ang} = \frac{1}{2n\sin\theta}\sqrt{\left[\left(\frac{\lambda}{T}\right)^2 - \left(\frac{\Delta n}{\cos\theta}\right)^2\right]}$$
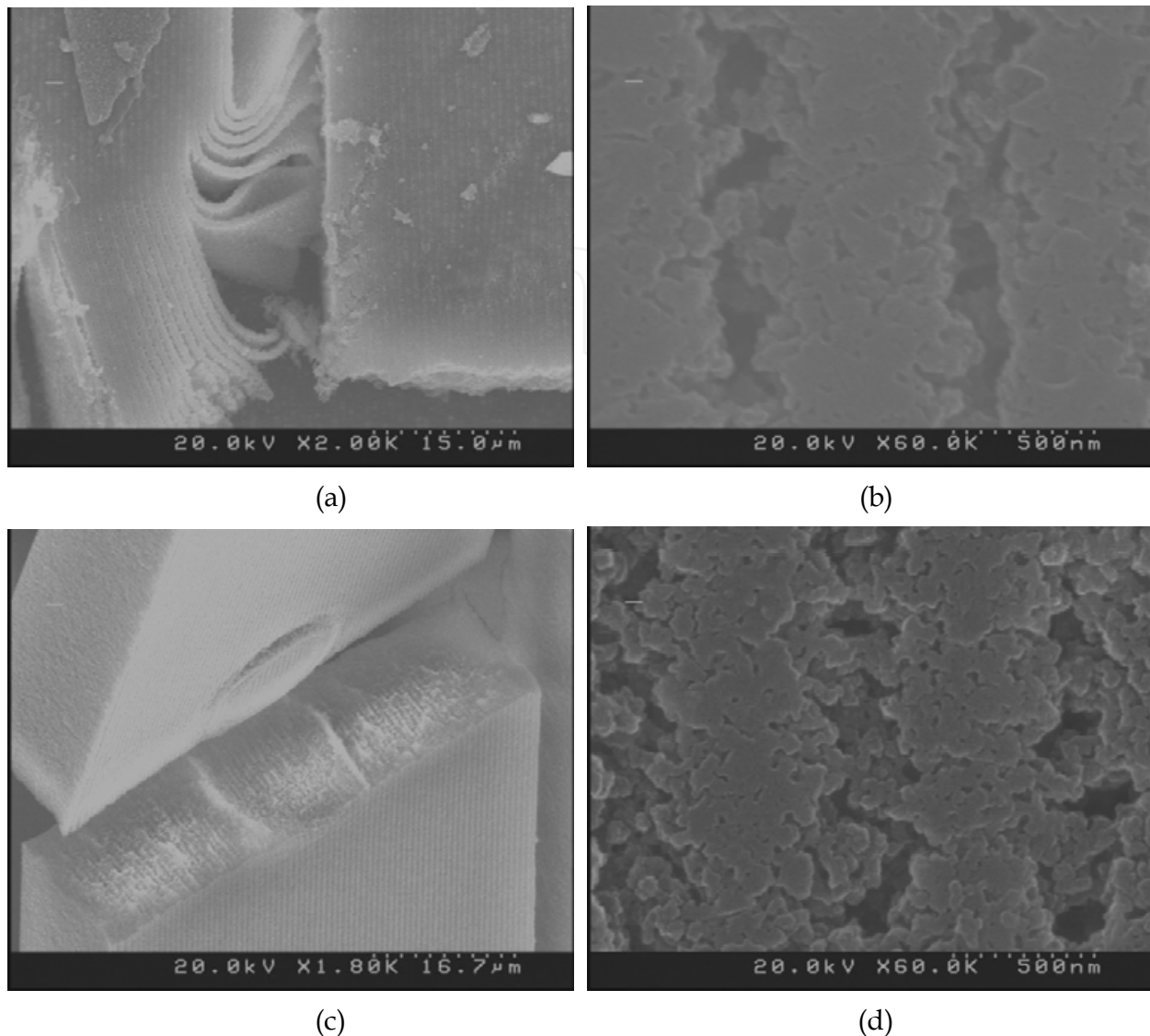
(2)

(a)

(b)

(c)

(d)

Fig. 9. SEM morphologies of gratings formed with H, TMPTA and various concentration of E7 [TMPTA : NVP: H = 50: 10: 40 relative wt %] (a) 5 wt %, (b) 5 wt %, ×60K, (c) 20 wt %, and (d) 20 wt %, ×60K.

where n is the average refractive index of recording solution, θ is the internal incident beam angle, T is the thickness of the hologram, λ is the recording wavelength, and n is the modulation of refractive index of the recording solution after recording.

Angular selectivity of our samples were similar, irrespective of the structures of epoxides (about 4˚) as typically shown in Figure 10. Solid line represents the simulated theory values according to the Kogelnik's coupled wave theory.

G. Montemezzani group reported that the use of Kogelnik's expression assuming fully symmetric beam geometries in highly birefringent materials such as LC leads to a large error [51]. Our experimental data showed only a little deviation from the theoretical values by the Kogelnik's coupled wave theory. This maybe attributed to the slight thickness reduction by small volume shrinkage still existing. The role of both factors should be clarified in the future.
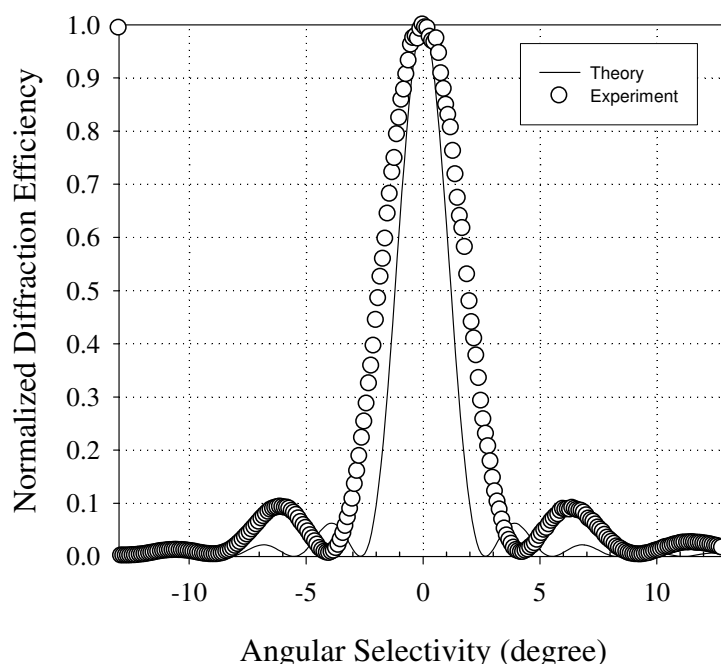
High Performance Holographic Polymer Dispersed Liquid Crystal Systems Formed
with the Siloxane-containing Derivatives and Their Applications on Electro-optics

607

Fig. 10. Angular selectivity of gratings formed with H , TMPTA, and 5 wt % E7 [TMPTA :
NVP : H = 50: 10: 40 relative wt %].

3.4 Effectiveness of M_M-TMOS on formation of holographic gratings

As a preliminary experiment, M_M-TMS and M_M-TMOS were compared as a diluent for the
polymer matrix component (totally 65 wt%, TMPTA : M_M-TMS, or M_M-TMOS : NVP = 10 :
80 : 10 in wt%, average double bond functionality = 1.1 on mole base), together with 35wt%
LC of TL203. As shown in Figure 11 gratings could not be formed with M_M-TMS even with
30 min irradiation of light, because of the low average functionality of the polymerization
system. G. P. Crawford reported that HPDLC gratings made with monomer mixtures with
average double bond functionality less than 1.3 were mechanically very weak[52]. In
general, it is difficult to form holographic gratings with low concentration of multi-
functional acrylate (average double bond functionality < 1.2) by dilution with mono-
functional component in radical polymerization.

Dramatic enhancing in the diffraction efficiency to about 86% (induction period of 144 sec)
was observed in case of M_M-TMOS, even with only 10 wt% TMPTA by using 0.2 wt% KC
and 2wt% DPI. Only trimethoxysilyl and trimethylsilyl parts are different in these two
formulations. Hydrolysis of trimethoxysilyl group by moisture and following condensation
seems responsible for the increased diffraction efficiency.

Effects of Alkyl and Spacer Groups in ω-Methacryloxyalkyltrialkoxysilanes on the
Formation and Performance of Gratings

In order to systematically study the influence of alkyl group and spacer group of ω-
methacryloxyalkyltrialkoxysilanes on the formation and performance of the formed
gratings, their chemical structures were modified as shown in Figure1. The relative
concentration was set as TMPTA : ω-methacryloxyalkyltrialkoxysilane : NVP = 10 : 80 : 10
wt% to clearly extract the effects of hydrolysis-condensation of trialkoxysilyl group on the
formation of the gratings and the performance of the formed gratings.

Figure 11 shows the real-time diffraction efficiency of holographic gratings formed with various ω-methacryloxyalkyltrialkoxysilanes capable of radical photo-polymerization and hydrolysis- condensation.

When spacer was changed from methylene to propylene (M_P-TMOS), the diffraction efficiency was dropped to 72% with longer induction period (576 sec). This seems to be because of the higher hydrophobicity of the spacer group compared with M_M-TMOS. The rate of the hydrolysis-condensation of trialkoxysilyl functions seems very important.

By changing the trialkoxysilyl functional group from trimethoxy to triethoxy (M_P-TMOS to M_P-TEOS) with the same propylene spacer, not only the diffraction efficiency was decreased to 13%, but the induction period was also elongated to 693 sec, which again strongly suggested that the hydrolysis-condensation process of trialkoxysilane function is playing an essential role in grating formation.

In grating formation, induction period basically depends on the time of the formation of cross-linked polymer matrix. In classical grating formation by radical polymerization of multi-functional acrylates, induction period is observed because polymerization does not start until the complete consumption of oxygen present in the system as an inhibitor. In the present system, the induction period depends on the actual gelation time of recording solution assisted by hydrolysis-condensation of trialkoxysilyl functions. The induction period varies by the physical property of ω-methacryloxyalkyltrialkoxysilane derivatives. The rate of the hydrolysis-condensation of trialkoxysilyl functions by moisture strongly depends on the hydrophobicity of the methacrylate monomer. Polymerization of recording solution leads to changes in the chemical potential of the system, and increases the miscibility gap between LC and polymerized matrix
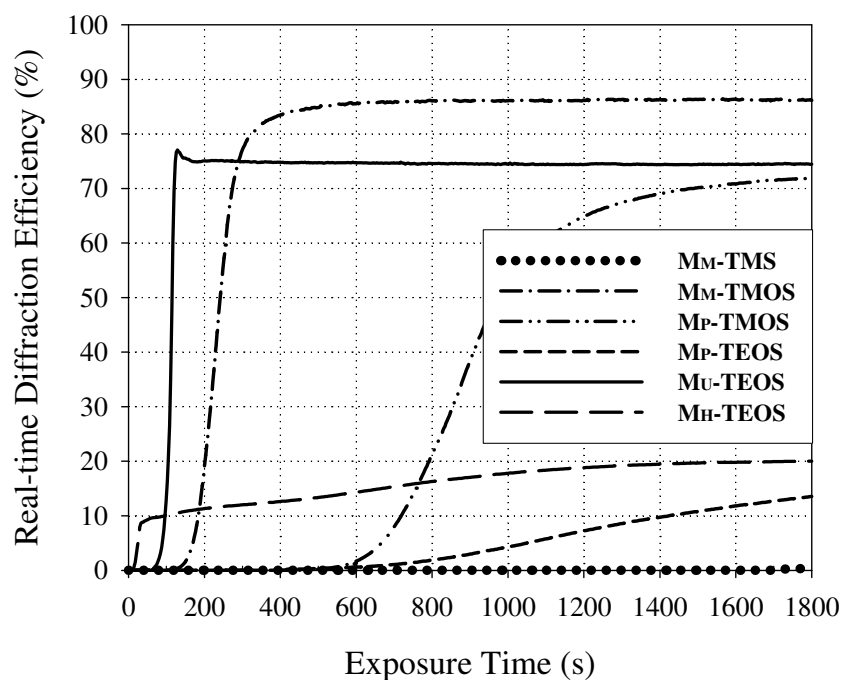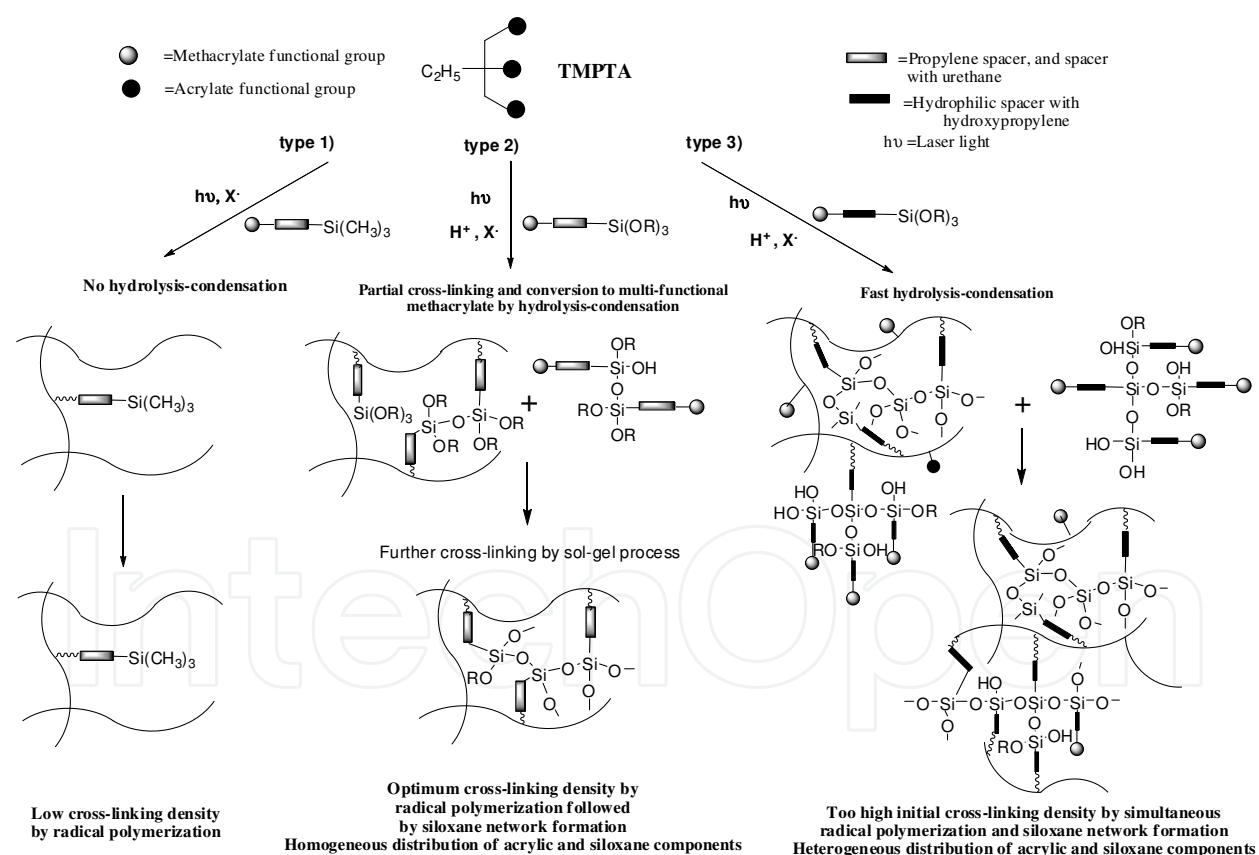

Fig. 11. Real-time diffraction efficiency of the gratings formed with various ω-methacryloxyalkyltrialkoxysilanes in the recording solution with 65 wt% matrix compounds of TMPTA : ω-methacryloxyalkyltrialkoxysilane : NVP = 10 : 80 : 10 wt% and 35 wt% TL203, and KC-DPI (0.2 wt% - 2 wt% to matrix compounds) with one beam intensity of 20 mW/cm².

To investigate the effects of chemical structures of spacer between trialkoxysilylalkyl group and methacrylate group, hydrophilic urethane and hydroxylpropylene groups were introduced in the spacer of the monomer structure. The highest diffraction efficiency of 75% and remarkably shorter induction period of 75 sec were obtained for grating formed with M_U-TEOS having urethane linkage in spacer group. In addition, gratings formed with M_H-TEOS having hydroxylpropylene group in the spacer showed the shortest induction period of 18 sec, although the diffraction efficiency was considerably low (20%).

To summarize the results, we may consider that the radically mono-functionally polymerizable 3-methacryloxypropyltrialkoxysilane became apparently multi-functional cross-linkable monomer by hydrolysis and condensation of trialkoxysilyl group as shown in Scheme 1, which induced the high concentration of cross-linking with moderate rate by the hydrolysis.

Scheme 1 proposed matrix formation processes: 1) radical cross-linking by TMPTA, 2) simultaneous radical cross-linking of TMPTA and small amounts of multi-functional methacrylate formed via hydrolysis-condensation of trialkoxysilyl group, followed by further cross-linking by hydrolysis, 3) competing rapid cross-linking of (meth)acrylate functions and sol-gel process of trialkoxysilane function, followed by further cross-linking by radical polymerization and sol-gel process.

Scheme 1. Proposed matrix formation processes: 1) radical cross-linking by TMPTA, 2) simultaneous radical cross-linking of TMPTA and small amounts of multi-functional methacrylate formed via hydrolysis-condensation of trialkoxysilyl group, followed by further cross-linking by hydrolysis, 3) competing rapid cross-linking of (meth)acrylate functions and sol-gel process of trialkoxysilane function, followed by further cross-linking by radical polymerization and sol-gel process.

In case of methacryloxymethyltrimethylsilane, cross-linking density is not high enough to form grating. This process corresponds to type 1) in Scheme 1. In TMOS or TEOS system, the hydrolysis of trialkoxysilyl group is relatively slow compared with the fast radical polymerization of TMPTA. Thus, grating formation is not rapid, but following cross-linking by hydrolysis assisted the formation of polymer matrix and further diffusion of LC to form gratings with high diffraction efficiency. By the introduction of urethane function in the spacer, the hydrophilic nature of the spacer increases the hydrolysis of triethoxysilyl group by moisture, and converts mono-functional methacrylate to apparently multi-fumctional methacrylate, and assisted the formation of polymer matrix by radical polymerization together with cross-linking by hydrolysis condensation. This process corresponds to type 2) in Scheme 1. In case of the introduction of hydroxypropylene spacer, too much hydrophilic nature of the spacer strongly enhanced the hydrolysis of the trialkoxysilyl group, and created the situation where apparently high concentration of multi-functional (meth)acrylates in the initial polymerization solution, and resulted in rapid formation of grating by radical cross-linking, but low diffraction efficiency. This process corresponds to type 3) in Scheme 1.

The spectral responses of the demultiplexer are measured by use of a broadband erbium-doped fiber amplifier (EDFA) source and are monitored by means of an optical spectrum analyzer for each channel. Figure 12 shows the spectra of the two output channels with the uniform gratings formed with M_U-TEOS at the ratio of TMPTA: M_U-TEOS: PI solution = 40: 50: 10 wt% (35 wt% of TL203 to monomer solution). All the channels had a 3-dB bandwidth of 0.13 nm and a channel spacing of 0.4 nm, and the interchannel cross-talk level, defined as the difference between the maximum power of a channel at the band edge and its power at the adjacent signal's band edge, is reduced by ~18dB.
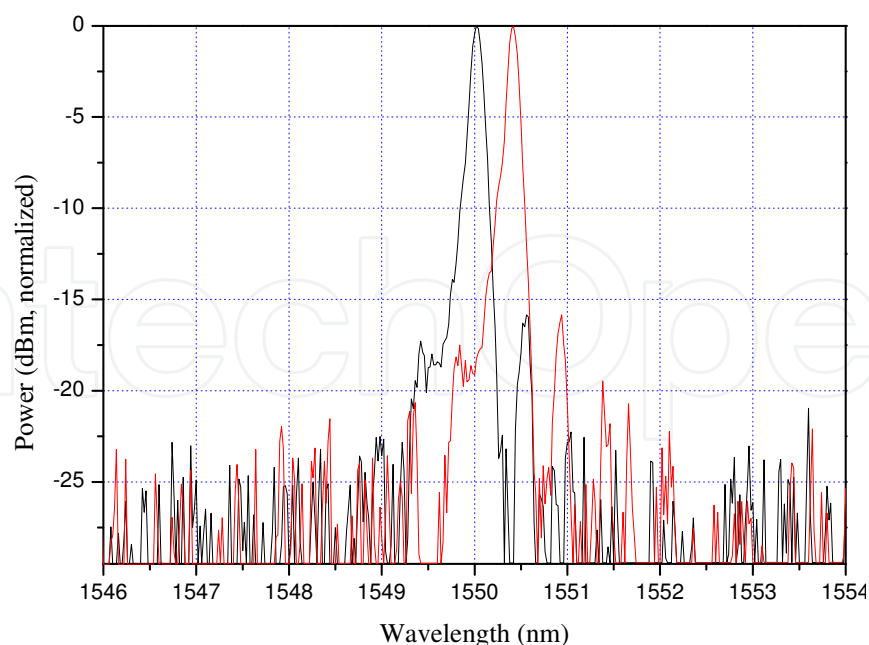

Fig. 12. Spectra of two output channels with 0.4 channel spacing for uniform gratings formed with M_U-TEOS at the ratio of TMPTA: M_U-TEOS: PI solution = 40: 50: 10 wt% (35 wt% of TL203 to monomer solution).

3.5 Effects of triethoxysilyl, hydroxyl, and methacrylate functional groups based on PPG derivatives on performance of holographic gratings

Figure 13 shows the AFM surface topology of the gratings formed with the formulation with 65 wt% polymer matrix compound of the ratio 20: 10: 50: 20 in TMPTA: NVP: Mu-TEOS: PPG-DTEOS and 35wt% of E7. Very regular and well-defined gratings were fabricated as shown in Figure 13(a) scanned in 10 μm length. The grating spacing was approximately 839.8 nm as shown in Figure 13(b) scanned in 3 μm length, which was in good agreement with the calculated spacing value of 965 nm by Bragg's equation (grating spacing $\Lambda = \lambda$ / $2\sin\theta$, λ is 532 nm wavelength of laser light and θ is 16 degree of incident external half angle in this experiment). Polymer matrix layers are shown as the sinusoidal pattern in profile of AFM topology since the LC layers were washed out by methanol from the positions of the valley parts in sinusoidal pattern, which maybe concluded that polymer matrix with PPG-DTEOS was exactly formed by photo-reaction in high intensity regions and E7 was phase-separated in low intensity regions of interference pattern of two laser beams.

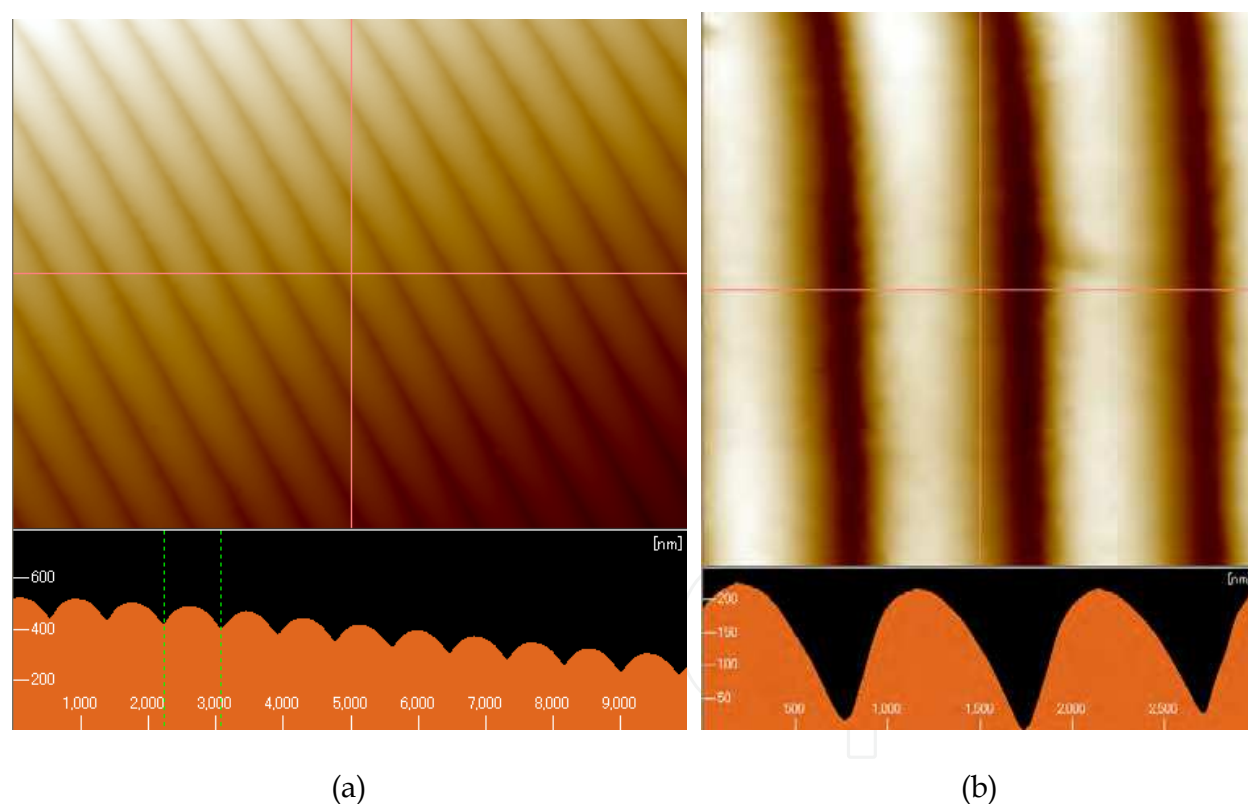(a)   (b)

Fig. 13. AFM surface topologies of the gratings formed with the formulation with 65 wt% polymer matrix compound of the ratio 20: 10: 50: 20 in TMPTA: NVP: Mu-TEOS: PPG-DTEOS and 35wt% of E7 in (a) 10 μm and (b) 3 μm scanning lengths.

The effectiveness of functional groups of PPG derivatives were observed on real-time diffraction efficiency as shown in Figure 14. Photo-reactive solutions (matrix components) were prepared from the ratios of 20: 10: 50: 20 wt% in TMPTA: NVP: Mu-TEOS: PPG

derivatives. Holographic recording solutions with E7 were ready to make holographic gratings in the ratio of 65 wt% and 35wt% as photo-reactive solutions and E7, respectively.

By changing the functional groups of PPG derivatives as triethoxysilyl, hydroxyl, and methacrylate groups, remarkable differences were observed on diffraction efficiency even though the induction periods for grating formation were similar with 33 second. The highest final diffraction efficiency of 93% was observed in holographic gratings formed from PPG-DTEOS with difunctional triethoxysilyl groups at 240 second of irradiation of light. In the case of PPG-HTEOS together with hydroxyl and triethoxysilyl groups, maximum diffraction efficiency was approximately 78%. When the PPG-MTEOS together with methacrylate and triethoxysilyl groups was used, maximum diffraction efficiency reached at 96% and gradually decreased to 60%. These phenomena may be considered that the functional groups of PPG derivatives affected strongly on the diffraction efficiency attributed to the difference of reaction kinetics and extend of LC phase separation. In the case of PPG-DTEOS and PPG-HTEOS, phase separation of LC should not be so fast compared with the case of PPG-MTEOS, and further cross-linking by the formation of siloxane network helped the LC to gradually phase-separate into low intensity regions of interference patterns, and maximum diffraction efficiency was reached at slower exposure time than PPG-MTEOS.
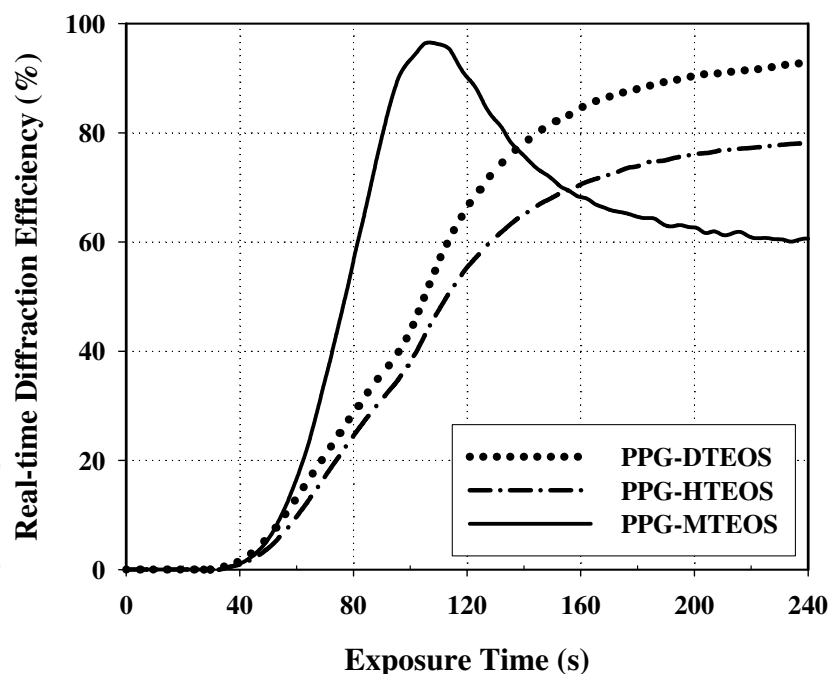

Fig. 14. Real-time diffraction efficiency of the gratings formed with PPG-DTEOS, PPG-HTEOS, and PPG-MTEOS in the recording solution with 65 wt% polymer matrix compounds of the ratios 20 : 10 : 50 : 20 wt% in TMPTA : NVP: Mu-TEOS: PPG derivatives, and 35 wt% E7.

4. Conclusion

We have demonstrated the effectiveness of the introduction of siloxane component to ring opening crosslinkable monomer as polymer matrix component to enhance the performance of HPDLC grating. High diffraction efficiency over 97% was obtained by using 1,3-bis(3-glycidoxypropyl)-1,1,3,3,5,5-hexamethyltrisiloxane (D), which induces a fast and good phase separation due to flexible and incompatible properties of siloxane component even at low concentration of E7 (10wt %). Gratings with much higher performance such as low volume shrinkage with 5.57% could be obtained in the case of 1,3-bis[2-(1,2-epoxycyclohex-4-yl)ethyl]-1,1,3,3-tetramethyldisiloxane (G).

Stable transmission holographic polymer dispersed liquid crystal gratings were efficiently prepared via network formation by radical polymerization of tri-functional acrylate assisted by hydrolysis-condensation reaction or trialkoxysilane functional group of ω-methacryloxyalkyltrialkoxysilane, induced by radical and proton species produced in the photo-decomposition of initiating system composed of 3, 3'-carbonylbis[7'-diethylaminocoumarine] as a photo-sensitizer and diphenyliodonium hexafluorophosphate as a photo-initiator.

The longest grating spacing of 0.9 μm indicated the least volume shrinkage.

At higher concentration of methacrylate, gratings formed with trimethoxysilylmethyl methacrylate capable of siloxane network formation showed remarkably higher diffraction efficiency than that formed with trimethylsilylmethyl methacrylate, which does not have functional groups to be cross-linked by hydrolysis

High diffraction efficiency of 72% was obtained in gratings formed with trimethoxysilylpropyl acrylate and **E7** (35wt%) with 0.2 wt% 3, 3'-carbonylbis(7-diethylaminocoumarin), and 1 wt% diphenyliodonium hexafluorophosphate. In SEM morphology, very regular and well-defined gratings were observed for the gratings formed with trimethoxysilylpropyl acrylate. Although gratings formed with high concentration of trimethoxysilylpropyl acrylate had some cracks in polymer matrix, the largest grating spacing was observed indicating the lowest volume shrinkage.

We developed a very useful holographic recording materials based on polypropylene glycol (PPG) derivatives functionalized with triethoxysilyl, hydroxyl, and methacrylate groups by taking into account the reaction rates and extent of phase separation of E7 of nematic LC in transmission holographic polymer dispersed liquid crystal (HPDLC) systems.

Holographic gratings were clearly formed from the radical polymerization and hydrolysis-condensation reaction of recording solution with PPG derivatives, which was demonstrated by AFM topology with very regular and well-defined morphology having the grating spacing of approximately 839.8 nm.

The highest final diffraction efficiency of 93% was observed in holographic gratings formed from PPG-DTEOS with difunctional triethoxysilyl groups at 240 second of irradiation of light. In the case of PPG-HTEOS together with hydroxyl and triethoxysilyl groups, maximum diffraction efficiency was approximately 78%. When the PPG-MTEOS together with methacrylate and triethoxysilyl groups was used, maximum diffraction efficiency reached at 96% and gradually decreased to 60%. These phenomena may be considered that

the functional groups of PPG derivatives affected strongly on the diffraction efficiency attributed to the difference of reaction kinetics and extend of LC phase separation.

Consequently, if I consider the structure and reactivity of siloxane compounds in relation with the property, it will be possible to propose new systems to improve the performance of HPDLC gratings. I believe that these novel recording materials controlled in nanometer scale can be significantly contributed to the development and progress in the optics, electronics, photo-induced patterning, microsystem, and nanotechnololgy. Especially, electrically switchable holographic gratings are very promising for actual application such as 3-D image storage, full color LC display, dense wavelength division multiplexing (DWDM), and polarization-selective element. Moreover, this research will contribute to the establishment of new-generation display or device technology and will encourage the activity of industries.

5. References

[1] Coufal, H. (1998). *Nature,* 393, 628.

[2] Heanue, J.F.; Bashaw, M.C. & Hesselink, L. (1994). *Science,* 265, 749.

[3] Shen, X.A.; Nguyen, A.; Perry, J.W.; Huestis, D.L. & Kachru, R. (1997). *Science,* 278, 96.

[4] Chilling, M.L.; Colvin, V.L.; Dhar, L.; Harris, A.L.; Schilling, F.C.; Katz, H.E.; Wysocki, T.; Hale, A.; Blyler, L.L. & Boyd, C. (1999). *Chem. Mater.* 11, 247.

[5] Park, M.S.; Kim, B.K. & Kim, J.C. (2003). *Polymer* 44(5), 1595.

[6] Meng, S.; Nanjundiah, K.; Kyu, T.; Natarajan, L.V.; Tondiglia, V.P. & Bunning, T.J. (2004). *Macromolecules*, 37, 3792.

[7] Meng, S.; Kyu, T.; Natarajan, L.V.; Tondiglia, V.P.; Sutherland, R. L. & Bunning, T.J. (2005). *Macromolecules*, 38, 4844.

[8] Kyu, T. & Nwabunwa, D. (2001). *Macromolecules*, 34, 9168.

[9] Pikas, D. J.; Kirkpatrick, S.M.; Tomlin, D.W.; Natarajan, L.; Tondiglia, V.P. & Bunning, T.J. (2002). *Appl. Phys. A*, 74, 767.

[10] Sutherland, R. L. (2002). *J. Opt. Soc. Am. B*, 19, 2995.

[11] Kato, K.; Hisaki, T. & Date, M. (1999). *Jpn. J. Appl. Phys.*, 38, 1466.

[12] White, T. J.; Natarajan, L. V.; Tondiglia, V. P.; Bunning, T. J. & Guymon, C. A. (2007). *Macromolecules*, 40, 1112.

[13] White, T. J.; Natarajan, L. V.; Tondiglia, V. P.; Lloyd, P. F.; Bunning, T. J. & Guymon, C. A. (2007). *Macromolecules*, 40, 1121.

[14] Kato, K.; Hisaki, T. & Date, M. (1999). *Jpn. J. Appl. Phys.*, 38, 805.

[15] Natarajan, L. V.; Brown, D. P.; Wofford, J. M.; Tondiglia, V. P.; Sutherland, R. L.; Lloyd, P. F. & Bunning, T. J. (2006). *Polymer*, 47, 4411.

[16] Jazbinsek, M.; Olenik, I.D.; Zgonik, M.; Fontecchio, A.K. & Crawford, G.P. (2001). *J. Appl. Phys.* 90(8), 3831.

[17] Zhang, J.; Carlen, C.R.; Palmer, S. & Sponsler, M.B. (1994). *J. Am. Chem. Soc.,* 116, 7055.

[18] Lucchetta, D.Ee.; Karapinar, R.; Manni, A. & Simoni, F. (2002). *J. Appl. Phys.*, 91, 6060.

[19] Choi, D. H.; Cho, M. J.; Yoon, H.; Kim, J. H. & Paek, S. H. (2004). *Opt. Mater.*, 27, 85.

[20] Jazbinsek, M.; Olenik, I.D.; Zgonik, M.; Fontecchio, A.K. & Crawford, G.P. (2001). *J. Appl. Phys.*, 90 (8), 3831.

[21] Zhang, J.; Carlen, C. R.; Palmer, S. & Sponsler, M. B. (1994). *J. Am. Chem. Soc.*, 116, 7055.

[22] Lucchetta, D. E.; Karapinar, R.; Manni, A. & Simoni, F. (2002). *J. Appl. Phys.*, 91, 6060.

[23] Rosa, M. E. D.; Tondiglia, V. P. & Natarajan, L. V. (1998). *J. Appl. Phys. Sci.*, 68, 523.

[24] Carretero, L.; Blaya, S.; Mallavia, R.; Madrigal, R. F. & Fimia, A. (1998). *J. Modern Opt.*, 45, 2345.

[25] Zhang, J. & Sponsler, M. B. (1992). *J. Am. Chem. Soc.*, 114, 1506.

[26] White, T.J.; Natarajan, L.V.; Tondiglia, V.P.; Lloyd, P.F.; Bunning, T.J. & Guymon, C.A. (2007). *Macromolecules*, 40, 1121-1127.

[27] Woo, J.Y.; Kim, E.H. & Kim, B.K. (2007). *J. of Polym. Sci.* A, 45, 5590-5596.

[28] Lee, L.H.; & Chen, W.C. (2001). *Chem. Mater*. 13, 1137.

[29] Yoshida, M. & Prasad, P.N. (1996). *Chem. Mater.* 8, 235.

[30] Murciano, A.; Blaya, S.; Carretero, L.; Acebal, P.; Perez-Molina, M.; Madrigal, R.F. & Fimia, A. (2008). *J. of Appl.Phys*, 104, 063109.

[31] Ramos, G.; Álvarez-Herrero, A.; Belenguer, T.; del Monte, F. & Levy, D. (2004). *Appl. Opt.*, 43, 4018-4024.

[32] Cho, Y. H.; Shin, C. W.; Kim, N.; Kim, B. K. & Kawakami, Y. (2005). *Chemistry of Materials*, 17,6263.

[33] Ohe, Y.; Kume, M.; Demachi, Y.; Taguchi, T. & Ichimura, K. (1999). *Polym. Adv. Technol*. 10, 544-553.

[34] Liu, Y. J.; Zhang, B.; Jia, Y. & Xu, K. S. (2003). *Opt. Commun.*, 218, 27.

[35] Sarkar, M. D.; Qi, J. & Crawford, G. P. (2002). *Polymer*, 43, 7335.

[36] Escuti, M. J.; Kossyrev, P. & Crawford, G. P. (2000). *Appl. Phys. Lett.*, 77, 4262.

[37] Cairns, D. R.; Bowley, C.C.; Danworaphong, S.; Fontecchio, A. K.; Crawford, G. P.; Li, L. & Faris, S. M. (2000). *Appl. Phys. Lett.*, 77, 2677.

[38] Bunning, T. J.; Liechty, W. B.; Natarajan, L. V.; Tondiglia, V. P.; Bunning, T. J. & Guymon, C. A. (2006). *Polymer*, 47, 2289.

[39] Cho, Y. H. & Kawakami, Y. (2005). *Silicon Chem.*, 3, 219.

[40] Gomurashvili, Z. & Crivello, J. V. (2002). *Macromolecules*, 35, 2962.

[41] Gomurashvili, Z. & Crivello, J. V. (2001). *J. Polym. Sci.: Part A: Polym. Chem.*, 39, 1187.

[42] Crivello, J. V. & Jiang, F. (2002). *Chem. Mater*. 14, 4858.

[43] Crivello, J. V. & Lam, J. H. W. (1997). *Macromolecules*, 10, 1307.

[44] Crivello, J. V. & Lee, J. L. (1989). *J. Polym. Sci.: Part A: Polym. Chem.*, 27, 3951.

[45] Castellanos, F.; Fouassier, J. P.; Priou, C. & Cavezzan, J. (1996). *J. Appl. Polym. Sci.*, 60, 705.

[46] Waldman, D.A.; Ingwall, R.T.; Dhal P.K.; Horner, M.G.; Kolb, E.S.; Li, H.-Y. S.; Minns, R.A. & Schild, H.G. (1995). *SPIE*, 2689, 127

[47] Rhee, U.S.; Caulfield, H.J.; Shamir, J.; Vikram, C.S. & Mirsalehi, M.M. (1993). *Opt. Engin.* 32(8), 1839.

[48] Mok, F.H. (1993). *Opt. Lett.* 18 (11), 915.

[49] Curtis, K.; Pu, A. & Psaltis, D. (1994). *Opt. Lett.,* 19(13).

[50] Kogelnik, H. (1969). *Bell Syst. Tech. J.*, 48, 2909.

[51] Montemezzani, G. & Zgonik, M. (1997). *Physical Review E*, 55(1), 1035.

[52] Sarkar, M.D.; Gill, N.L.; Whitehead; J.B. & Crawford; G.P. (2003). *Macromolecules*, 36, 630.
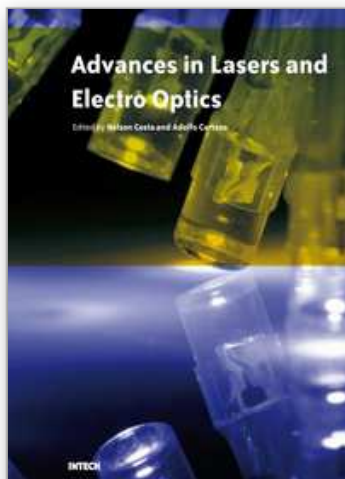
Advances in Lasers and Electro Optics

Edited by Nelson Costa and Adolfo Cartaxo

ISBN 978-953-307-088-9

Hard cover, 838 pages

Publisher InTech

Published online 01, April, 2010

Published in print edition April, 2010

Lasers and electro-optics is a field of research leading to constant breakthroughs. Indeed, tremendous advances have occurred in optical components and systems since the invention of laser in the late 50s, with applications in almost every imaginable field of science including control, astronomy, medicine, communications, measurements, etc. If we focus on lasers, for example, we find applications in quite different areas. We find lasers, for instance, in industry, emitting power level of several tens of kilowatts for welding and cutting; in medical applications, emitting power levels from few milliwatt to tens of Watt for various types of surgeries; and in optical fibre telecommunication systems, emitting power levels of the order of one milliwatt. This book is divided in four sections. The book presents several physical effects and properties of materials used in lasers and electro-optics in the first chapter and, in the three remaining chapters, applications of lasers and electro-optics in three different areas are presented.

INTECH
open science | open minds